Electronic Supplementary Material (ESI) for ChemComm.

Supporting Information

ZnO-Au@ZIF-8 Core-shell Nanorod Arrays for ppb-level NO_2 Detection

Mingqi Sun[#,a], Mingyuan Wang[#,b], Xin Ni[c], Guiwu Liu[a], Guanjun Qiao[a], Shuangying Lei[b], Mingsong Wang[*,a], Ling Bai [*,a]

[a]*School of Materials Science and Engineering, Jiangsu University, Zhenjiang, Jiangsu Province 212013, China*

[b]*SEU-FEI Nano-Pico Center, Key Laboratory of MEMS of Ministry of Education, School of Electrical Science and Engineering, Southeast University, Nanjing, Jiangsu Province 210096, China*

[c]*Department of Gastroenterology, Affliated Hospital of Jiangsu University, Zhenjiang, Jiangsu Province 212013, China*

[#]The authors contribute equally

*Corresponding authors.

E-mail addresses: wangms@ujs.edu.cn (M. Wang); lingmubai@ujs.edu.cn (L. Bai).

Author Contributions

Mingqi Sun: Conceptualization, Methodology, Formal analysis, Writing-original draft. **Mingyuan Wang:** Calculation, simulation. **Xin Ni:** Formal analysis. **Guiwu Liu:** Conceptualization. **Guanjun Qiao:** Methodology. **Shuangying Lei:** Methodology. **Mingsong Wang:** Methodology, Formal analysis. **Ling Bai:** Writing-review & editing.

1. Experimental

1.1. Chemical materials

The Pt-printed alumina substrate was described elsewhere [1]. The following chemicals: zinc acetate hydrate ($ZnAc_2 \cdot 2H_2O$, AR), zinc nitrate hexahydrate ($Zn(NO_3)_2 \cdot 6H_2O$, AR), ethanolamine (99 %), hexamethylenetetramine (HMTA, AR), N,N-dimethylformamide (DMF, AR), 2-methylimidazole (2-MeIM, 99 %), tetrachloroamic acid tetrahydrate ($HAuCl_4 \cdot 4H_2O$, AR), ethanol (99 %) and deionized water (H_2O) (Laboratory preparation) were purchased from Sino Chem Co., Ltd. China, and used directly as received without further purification and treatment.

1.2. Preparation of the ZnO and ZnO-Au nanorod arrays

ZnO nanorod arrays on alumina substrate were synthesized by a modified seed-assisted hydrothermal method. ZnO seed layer was deposited on the conductive side of the substrate by immersing it in the precursor solution, and withdrawn with a speed of 100 mm/min [2]. Then the substrate with ZnO seeds was placed in a 50 mL Teflon-lined stainless autoclave with the seeded side facing down, and 40 mL aqueous solution containing $Zn(NO_3)_2 \cdot 6H_2O$ (0.48 g) and HMTA (0.22 g) was added. The reaction was carried out at 120 ℃ for 100 min, and cooled to room temperature. For the ZnO-Au nanorod sample, 0.135mL $HAuCl_4 \cdot 4H_2O$ (10 mg/mL) was added into the aqueous solution during immersion. The above-synthesized products were washed repeatedly with deionized water and dried at 60 °C overnight. The ZnO and ZnO-Au composites were obtained by annealing at 400 ℃ for 5 h.

1.3. Preparation of the ZnO@ZIF-8 and ZnO-Au@ZIF-8 core-shell nanorod arrays

The ZnO@ZIF-8 and ZnO-Au@ZIF-8 core-shell nanorod arrays were prepared via a hydrothermal route similar with the reported study [3]. The as-prepared ZnO and

ZnO-Au nanorods grown on the alumina substrate and 2-methylimidazole (0.82 g, 0.5 M) were successively added to a Teflon-lined autoclave (25 mL) containing a mixed solvent of DMF and H_2O (20 mL, V_{DMF}: V_{H2O}=1:1), and heated at 60 °C for 10 min. After cooling to room temperature, the product was obtained and washed with fresh DMF and H_2O several times, and dried at 60 °C overnight.

1.4. Characterization

The morphologies and structures of the samples were characterized by scanning electron microscopy (SEM, FEI Nova Nano 450) and transmission electron microscopy (TEM, JEOL JEM-2100F at 200 kV). The crystalline structure and phase of the products were investigated by grazing incidence X-ray diffraction (GIXRD) on a Smartlab 9kw X-ray with Cu Kα radiation at λ =0.145 nm. The elemental valence states of the samples were determined via XPS equipment (Thermo Scientific K-Alph) and C1s peak at 284.8 eV was used as the calibration value of binding energy shift.

The details of the gas sensing performance of ZnO-based materials were described in the previous study. Under the preset gas concentration and heating temperature (125 ℃), the computer could monitor the resistance of the sensor. The sensor response is defined as the ratio of Rg/Ra (Ra/Rg) used to test oxidation (reduction) gas, where Ra is the resistance of the sensor in dry air and Rg is the resistance of the sensor in target gas. The response time and recovery time respectively correspond to the time required to obtain 90 % of the response, while the recovery time indicates the time required for the signal to recover to 90 %.

2. Supplementary Results

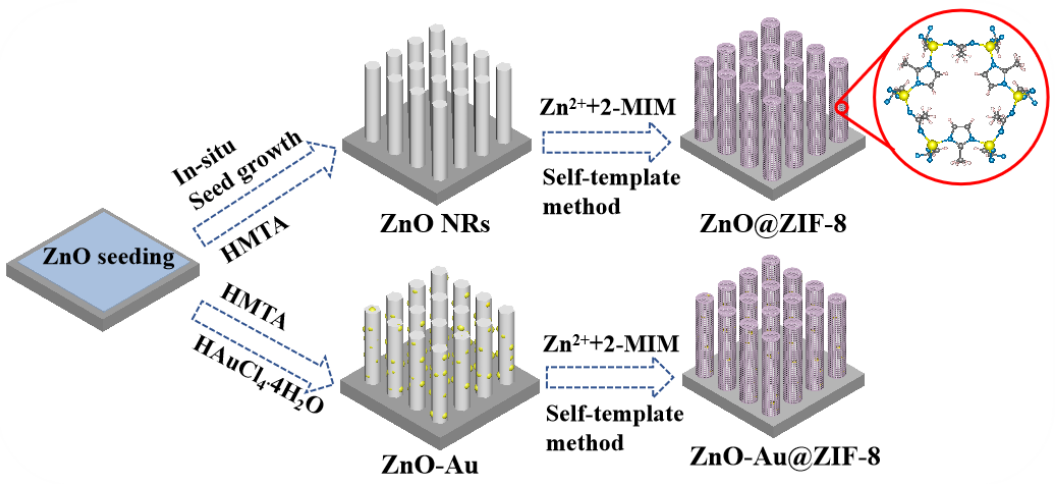

Fig. S1. Schematic diagram of the preparation of the ZnO@ZIF-8 and ZnO-Au@ZIF-8 core-shelled materials.

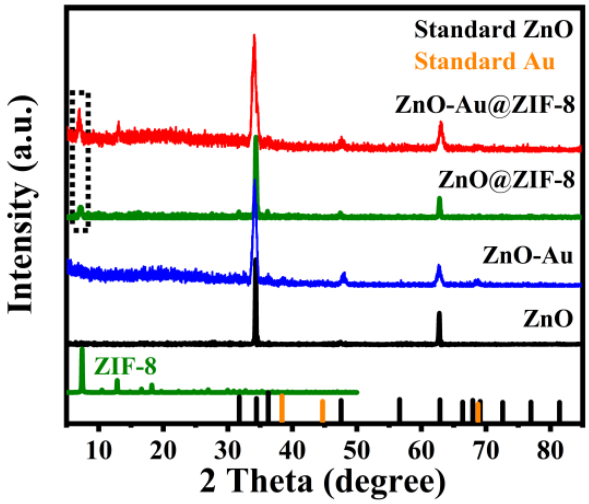

Fig. S2. The XRD patterns of (a) ZnO (black); (b) ZnO-Au (blue); (c) ZnO@ZIF-8 (green); (d) ZnO-Au@ZIF-8 (red) samples, respectively.

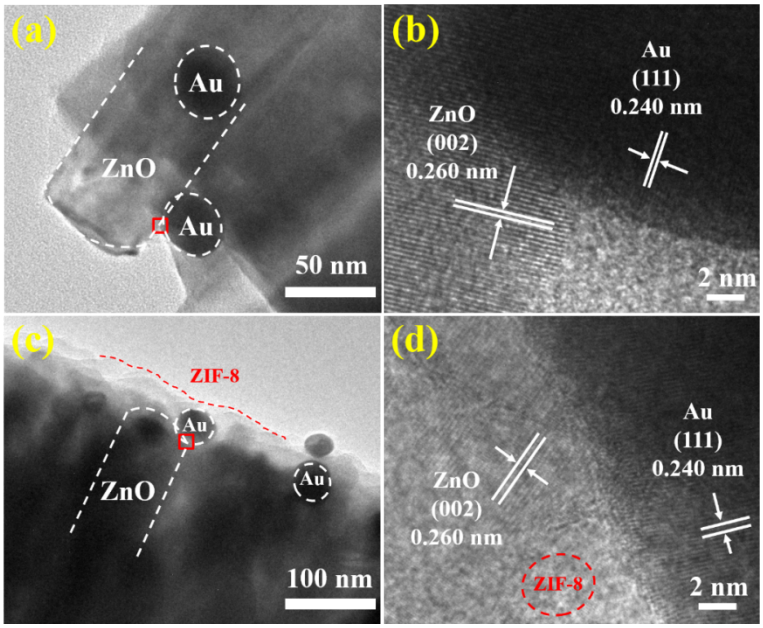

Fig. S3. The TEM and HRTEM images of (a,b) ZnO-Au and (c,d) ZnO-Au@ZIF-8 samples.

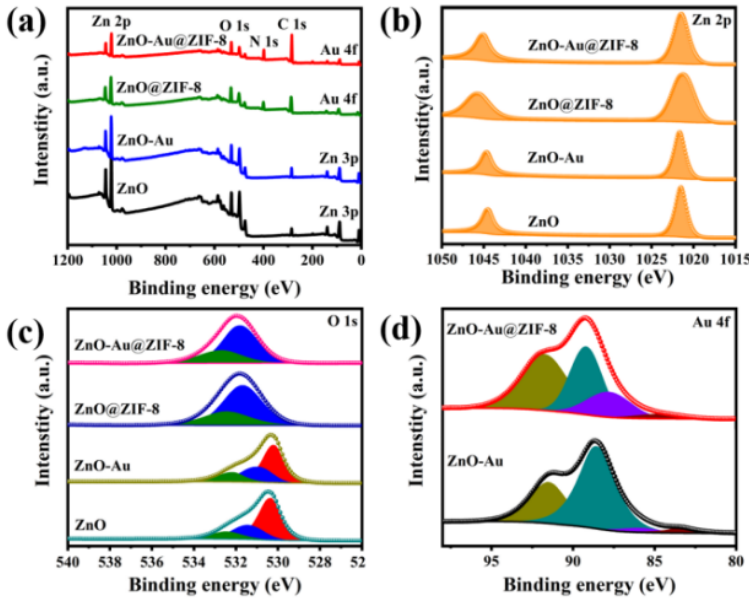

Fig. S4. XPS spectra of various samples: (a) survey spectrum, (b) Zn 2p, (c) O 1s and (d) Au 4f spectra.

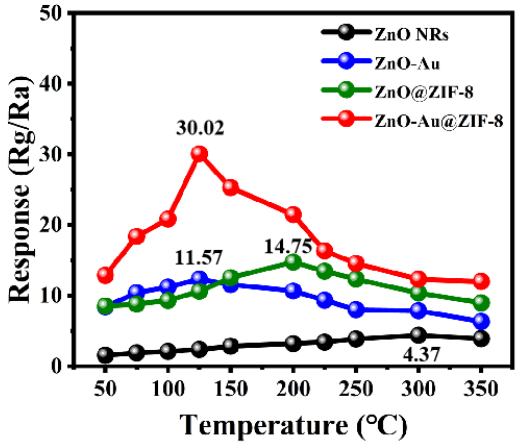

Fig. S5. The response of ZnO NRs, ZnO-Au, ZnO@ZIF-8 and ZnO-Au@ZIF-8 sensors to 1 ppm NO_2 obtained at various operating temperatures.

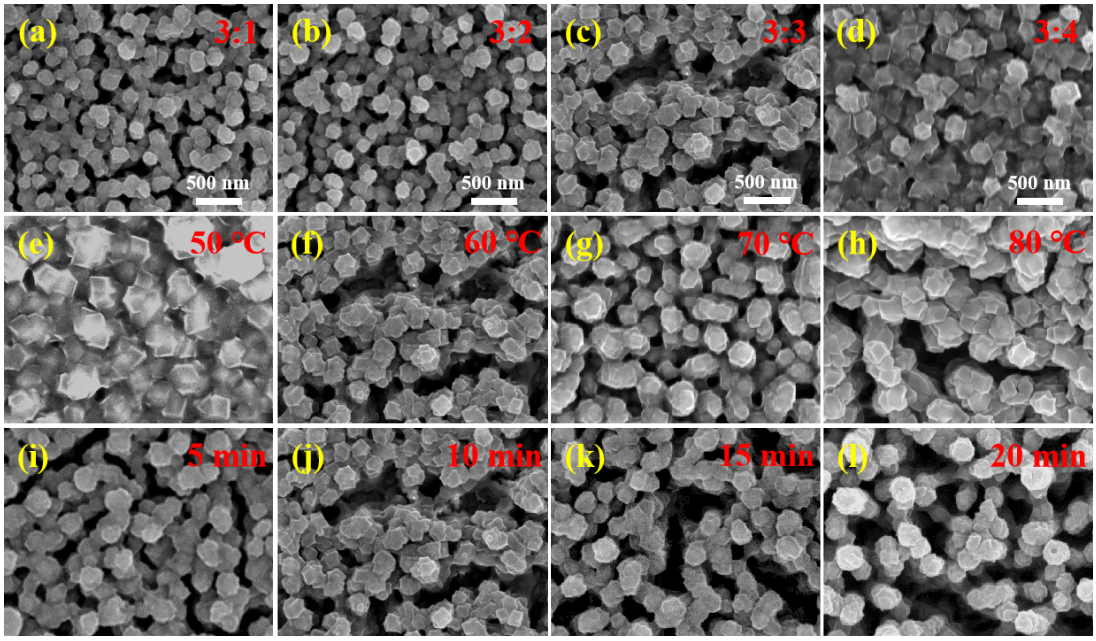

Fig. S6. The SEM images of ZnO@ZIF-8 composite films obtained with different DMF/ H_2O volume ratios: a) 3:1; b) 1:1; c) 1:3; d) 3:4 (T= 60 ℃, 10 min); ZnO@ZIF-8 composite films obtained at different reaction temperature: e) 50 ℃; f) 60 ℃; g) 70 ℃; h) 80 ℃ (DMF/ H_2O=1:1, 10 min); ZnO@ZIF-8composite films obtained at different reaction time: i) 5 min; j) 10 min; k) 15 min; l) 20 min (T= 60 ℃, DMF/ H_2O=1:1).

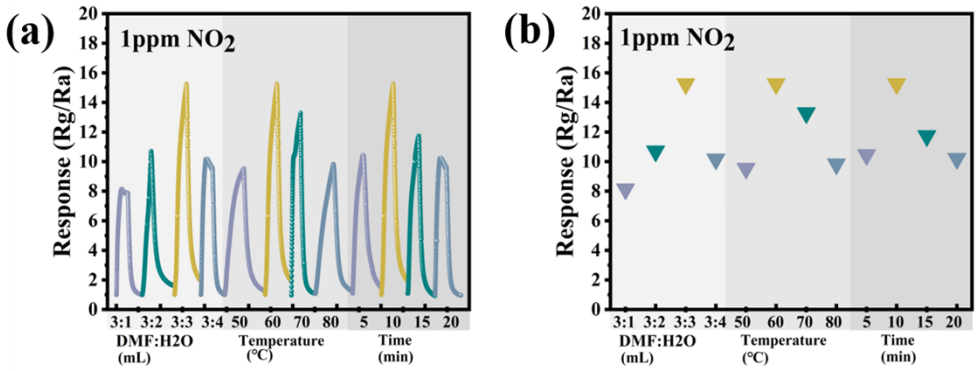

Fig. S7. The response of ZnO@ZIF-8 composite films obtained with different test conditions to 1 ppm NO_2.

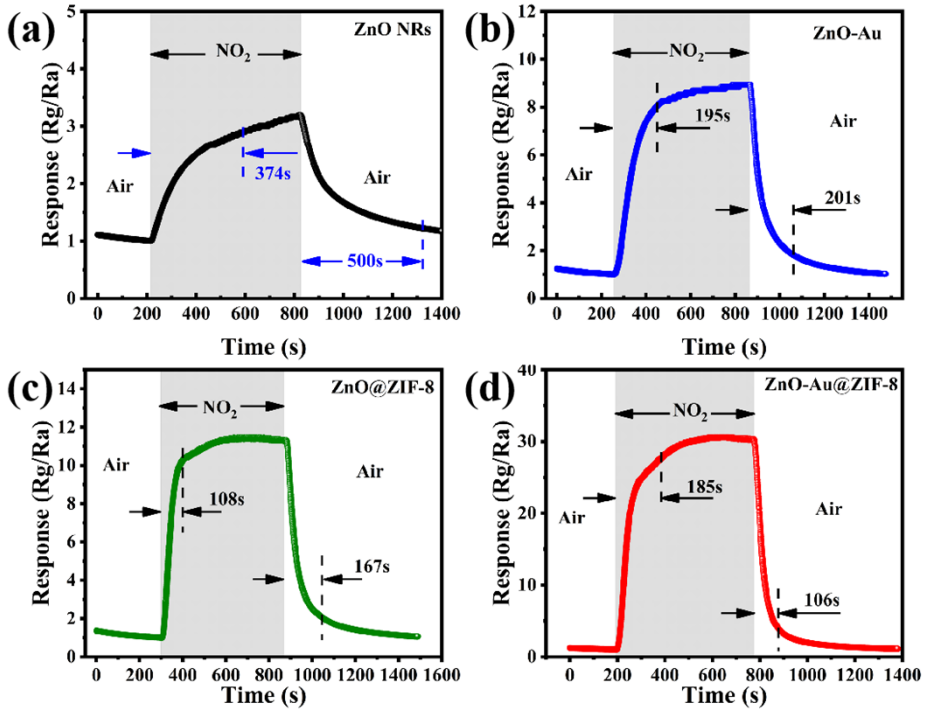

Fig. S8. (a-b) The dynamic response curves of ZnO NRs, ZnO-Au, ZnO@ZIF-8 and ZnO-Au@ZIF-8 sensors to 1 ppm NO_2 at 125 ℃.

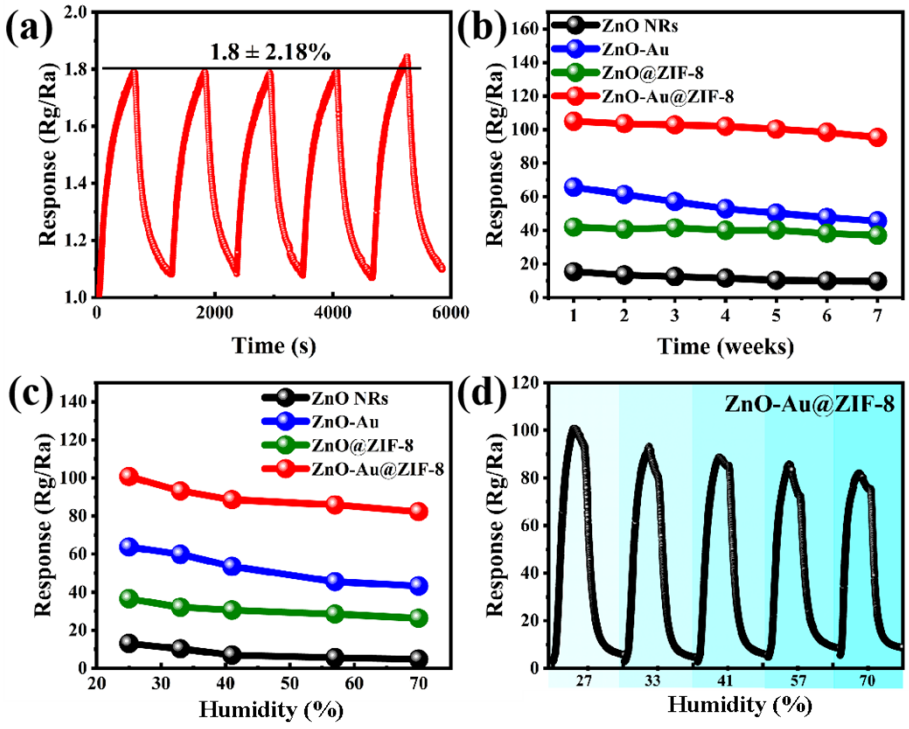

Fig. S9. (a) Repeatability test for ZnO-Au@ZIF-8 exposing to five-cycle 5 ppb NO_2 at 125 ℃; (b) long-term reliability test toward 10 ppm NO_2 within 50 days for four ZnO-based sensors; (c) the responses to 10 ppm NO_2 for the four ZnO-based sensors under various RH levels; (d) dynamic response curve toward 10 ppm NO_2 for ZnO-Au@ZIF-8 at 125 ℃ under different humidity conditions.

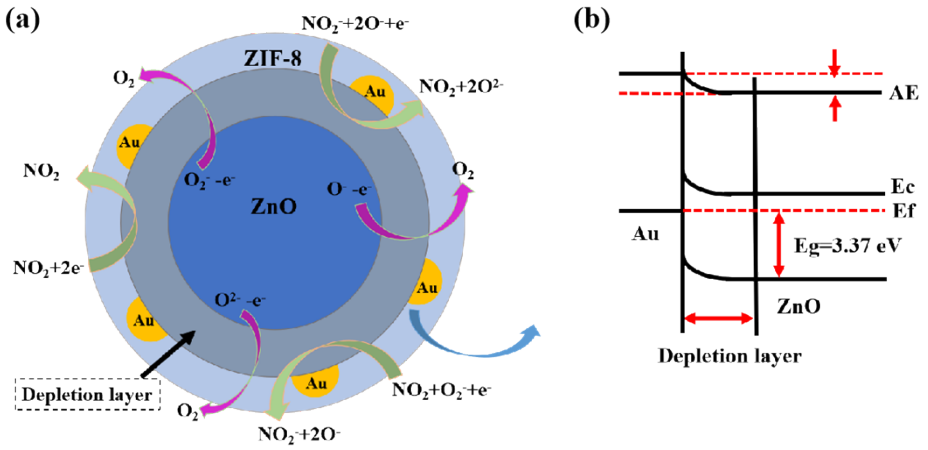

Fig. S10. Schematic illustration of the NO_2 sensing mechanism of ZnO-Au@ZIF-8 core-shell structure.

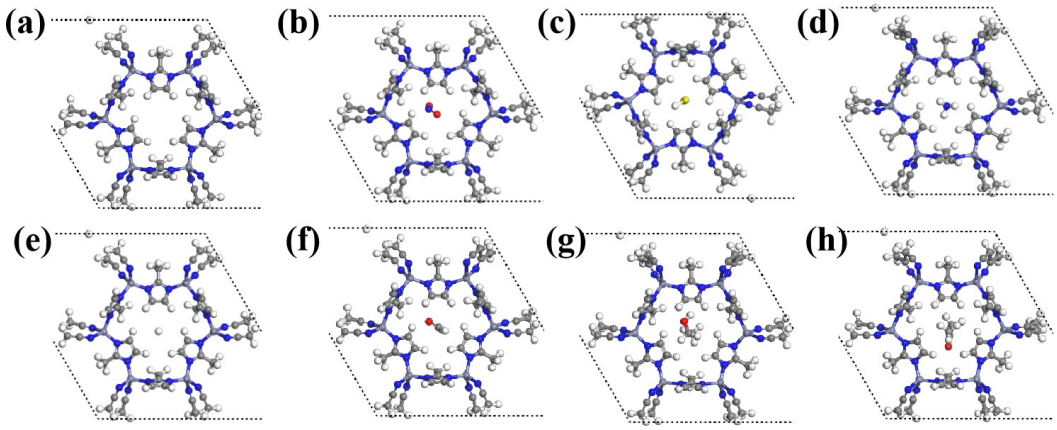

Fig. S11. (a) ZIF-8 intercepts molecular adsorption fragments; the theoretical binding configurations of different gas molecule on ZIF-8: (b) NO_2 on ZIF-8, (c) H_2S on ZIF-8, (d) NH_3 on ZIF-8, (e) H_2 on ZIF-8, (f) HCHO on ZIF-8, (g) CH_2CH_2OH on ZIF-8, (h) H_3CCOCH_3 on ZIF-8. The white, gray, red, blue, and yellow spheres represent H, C, O, N, and S atoms, respectively.

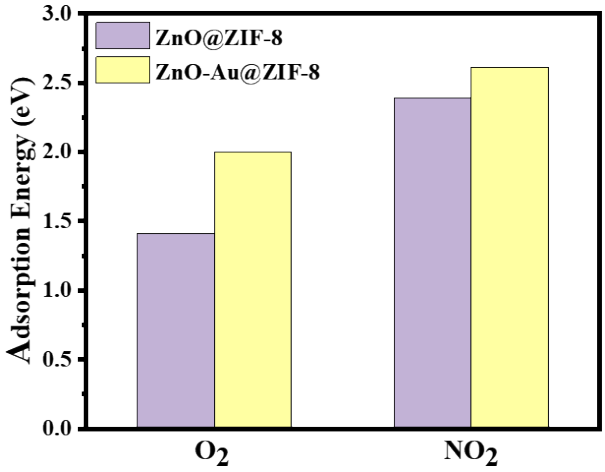

Fig. S12. Calculated adsorption energies of O_2 and NO_2 at ZnO@ZIF-8 and ZnO-Au@ZIF-8, respectively.

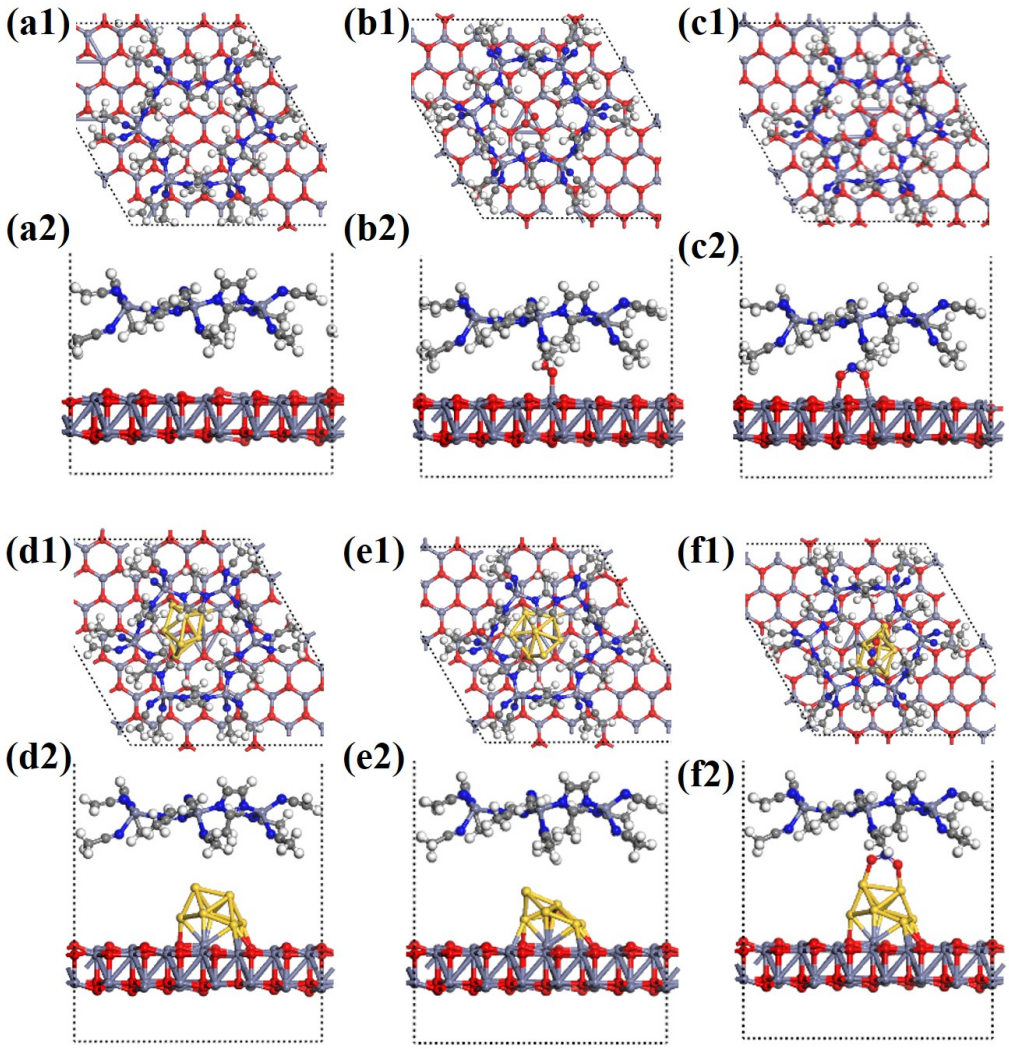

Fig. S13. Top and side views of the configurations for (a1, a2) ZnO@ZIF-8 composite, (b1,b2) O_2-adsorbed ZnO@ZIF-8 composite, (c1,c2) NO_2-adsorbed ZnO@ZIF-8 composite, (d1,d2) ZnO-Au@ZIF-8 composite, (e1,e2) O_2-adsorbed ZnO-Au@ZIF-8 composite, (f1,f2) NO_2-adsorbed ZnO-Au@ZIF-8 composite, obtained by DFT calculations. The white, gray, red, blue, purple and yellow spheres represent N, H, O, C, Zn and Au atoms, respectively.

Samples	O_L	O_V	O_C
ZnO	530.32 eV/57.99%	531.44 eV/25.58%	532.43 eV/16.43%
ZnO-Au	530.17 eV/52.67%	530.91 eV/29.08%	532.13 eV/18.45%
ZnO@ZIF-8	/	531.56 eV/69.98%	532.38 eV/30.02%
ZnO-Au@ZIF-8	/	531.8 eV/68.62%	532.68 eV/31.38%

Table S1. Different proportion of deconvoluted oxygen components in the ZnO, ZnO-Au, ZnO@ZIF-8, and ZnO-Au@ZIF-8 samples, respectively.

Sensing materials	Concentration	Work temperature	Sensor response（Rg/Ra）	References in the SI
ZnO-Au nanowires	1 ppm	250 ℃	51.01	4
ZnO/Au	5 ppm	Room temperature with UV illumination	0.6	5
ZnO@Pt nanowire	20 ppm	220 °C	7.01	6
Au/Pd–ZnO	5 ppm	100 ℃	732.4	7
ZnO-Au nanorods	5 ppm	300 ℃	1.2	8
Au nanoparticle decorated ZnO@ZIF-8 core-shell NRs	0.05 ppm	Room temperature with UV illumination	260 %	10
ZnO-Au@ZIF-8	5 ppm 5 ppb	125 °C	63.1 1.8	This work

Table S2. Comparison of NO_2 gas-sensing performance of various heterostructures.

References

1, M. S. Wang, Y. W. Wang, X. J. Li, C. X. Ge, S. Hussain, G. W. Liu, G. J. Qiao, Sens. Actuators B Chem., 2020, 8, 128050.

2, C. M. Chang, M. H. Hon, I. C. Leu, Sens. Actuators B Chem., 2010, 11, 15-20.

3, S. S. Nair, N. Illyaskutty, B. Tam, A. O. Yazaydin, K. Emmerich, A. Steudel, T. Hashem, L. Schöttner, C. Wöll, H. Kohler, H. Gliemann, Sens. Actuators B Chem., 2020, 2, 127184.

4, E. Navarrete, F. Güell, P. R. Martínez-Alanis, E. Llobeta, J. Alloys Compd., 2021, 890, 161923.

5, A.Gaiardo, B. Fabbri, A. Giberti, V. Guidi, P. Bellutti, C. Malagù, M. Valt, G. Pepponi, S. Gherardi, G. Zonta, A. Martucci, M. Sturaro, N. Landini, Sens. Actuators B Chem., 2016, 237, 1085-1094.

6, C. Y. Wang, J. Y. Xie, X. Chang, W. Zheng, J. Zhang, X. H. Liu, Chem. Eng. J., 2023, 473, 145481.

7, X. X. Chen. Y. F. Ouyang, T. H. Liu, C. Y. Zhang, S. Y. Huang, H. R. Shang, H. Lin, S. K. Zhao, Y. B. Shen, Vacuum, 2024, 219, 112742.

8, P. Rai, Y. S. Kim, H. M. Song, M. K. Song, Y. T. Yu, Sens. Actuators B Chem., 2012, 165, 133-142.

9, M. M. Zhan, C. X. Ge, S. Hussain, A. S. Alkorbi, R. Alsaiari, N. A. Alhemiary, G. J. Qiao, G. W. Liu, Chemosphere, 2022, 291, 132842.

10, T. Murugesan, R. R. Kumar, A. Ranjan, M. Y. Lu, N. H.Lin, Sens. Actuators B Chem, 2024, 402, 135106.